DESIGN APPROCH AND PERFORMANCE ANALYSIS OF A TRUNCATED IDEAL CONTOUR PROPULSION NOZZLE

Nahla BOUGHAZI[1], Abdelkrim HADDAD[1] & Hakim KBAB[2]

Propulsion nozzles generate the thrust needed through the conversion of thermal energy into kinetic energy. The combustion or working gases expansion takes place within the convergent, throat and divergent sections reaching supersonic velocities. The widely used contoured (or bell) geometry has been and is still popular because of its shorter length that leads to lesser mass along with its ability to direct the exhaust gases towards the axis of symmetry at the exit cross-section leading to greater thrust. The development of the present design procedure lies on three main phases starting with the design of an Ideal Contour (IC) divergent supersonic section using a home developed computer program integrating the method of characteristics (MoC) and simulating the divergent section as a 2nd-order polynomial then truncating it at a cross-section ratio that almost keeps its thrust and further reduces its mass. This would lead to the Truncated Ideal Contour (TIC) that is linked, to a convergent subsonic section designed using the method of Rao. The present study simulates both the (IC) and the (TIC) flow fields, and the results obtained in terms of both the pressure and Mach distributions along the centerline and the wall as well as the diverse performances represented by the developed thrust, the thrust coefficient and the specific impulse. In addition, the TIC profile was submitted to CFD analysis using the Ansys-Fluent Platform and all the results obtained, whether for the IC or the TIC configurations, are compared to similar results available in the specialized literature. Good agreement was achieved between the several components of the study.

Key-words: Truncated Ideal Contour (TIC) nozzle, Ideal contour (IC) nozzle Supersonic propulsion nozzles, MoC, CFD.

1. Introduction

It is Carl Gustaf Patrik de Laval who first developed the apparatus represented by a convergent-divergent pipe that led to the expansion of steams consequently increasing their velocity to supersonic speeds [1]. A supersonic nozzle (or de Laval nozzle) is a convergent-divergent device that is positioned between the combustion chamber and the external environment in order to obtain a mass flow

[1] Applied Mechanics of New Materials Laboratory-LMANM, Faculty of Science and Technology, Université 8 Mai 1945, Guelma-24000, Algeria
[2] Institute of Aeronautics and Space Studies, Université Saad Dahlab, Blida-1- 09000, Algeria

rate needed for the propulsion [2]. It accelerates the combustion gases to speeds higher than that of the sound and equips nowadays all aircraft and rocket engines. The gases are expanded as a result of the conversion of the thermal energy into kinetic energy, and the simulation of a propulsion nozzle operation is necessary to the understanding of the process that takes place within its contour as they move through the convergent section, the throat and the divergent section where the speed of the gas increases progressively while its pressure and temperature decrease. Over the past decades, several nozzle configurations have been proposed with the purpose of achieving a maximum thrust within a minimum length in order to decrease the mass. Such configurations include ideal, conical, bell, plug, expansion-deflection, dual bell, and multi grid profiles. An interesting review of rocket nozzle development over the last seven decades has been performed by Khare and Saha [3].

Apart from the conical nozzle that that has been applied in early rocket engines development, almost all nozzle configurations had their contour designed with the help of the MoC. Ease and flexibility to be manufactured in diverse area ratios constitute the main advantage of the conical configuration. The contour is a straight line with commonly a 15° divergent angle. However, it is much restrained in terms of weight and performance loss at low altitude [4]. Contoured or Bell-type nozzles however, with their high angle of expansion established at 20°-50° right downstream of the throat and a 5°-10° half angle at the exit lip achieved through a gradual reversal of the contour slope are approximately 20% shorter in length and consequently lighter [2].

The design of such nozzles to a required exit Mach number necessitates the application of the MoC that reduces the system of partial differential equations representing the governing equations into a system of ordinary total differential equations represented by the characteristic and the compatibility relationships. The computations are carried out through a step-by-step procedure along the Mach lines which physically represent the direction of propagation of a perturbation in the flow-field. These characteristics, from a more rigorous point of view, are illustrated by the curves on which the partial differential equations describing the flow are reduced to an internal operator represented by the ordinary differential compatibility equation [5]. The implementation of the MoC was initially performed within the NASA's Lewis Research Center in Cleveland, Ohio and the analytical solution led to the design of wind tunnel nozzles [6].

A computer program that establishes the method integrating a practical approach to the design of supersonic nozzles along with a method for the computations of the transonic flow parameters needed to start it at the throat was later developed and published at Purdue University, USA [7]. Using the MoC, a minimum length nozzle contour was designed through reducing its expansion region length rending it lighter and more efficient for operations [8]. Later on, a

Matlab function has been employed to plot all the characteristic and contour wall points in order to produce the final nozzle geometry that may be drawn. A commercial CFD package was later applied to simulate the flow field within the configuration designed and showed the effectiveness of the approach. Imposing both the wall expansion angle and the exit Mach number, a minimum length nozzle that achieves Mach 3 has been designed and the results obtained compared to those of the well-known 1-D approach. A truncation was then performed to obtain a TIC contour of x/r_t=13.4. It was further compressed (CTIC) attaining x/r_t=12.6 where (r_t) represents the radius at the throat. The TIC nozzle produced showed a thrust coefficient of C_T=1.64 and an exit Mach number of 2.47-2.72 depending if it is at the wall or centerline rather than Mach 3 as a result of the shortened straightening section. A development of the MoC in 3D was attempted, applied and the obtained results that have been compared to its 2D counterpart [9].

A C-program based on the MoC and streamline function was developed and applied for the definition of a nozzle contour for cold flow (represented by air at 300K) and hot flow (hydrogen at 1000K) for an outlet Mach number of 3. A CFD analysis was likewise performed for the 2D axisymmetric flow in the bell-type nozzle at design and non-design conditions. CFD software Gambit 2.4.6 and Fluent 6.3.26 were employed. The authors [10] succeeded in locating the normal shock wave and observed an agreement between the 1-D analytical results and those predicted by the CFD simulation in terms of structure, location and size. A comparable approach has been applied [11] in 2D and used to design the nozzle of a Shcramjet engine and optimize it in terms of flow and geometric parameters. The MoC was used to obtain five 2D geometries through varying the slant angle of the initial characteristic line from -5° to 14° and expanding the combustion gases from the pressure of 8 bars to atmospheric at an altitude of 32.5 km i.e. 0.015 bar. Mach 12.5 was achieved with the largest nozzle (i.e. at slant angle -5°) showing a better performance than the smallest ones at slant angles of 0°, 5°, 10° and 14°. The MoC has also been integrated in a Matlab code and applied to obtain the contour of the divergent sections that accelerates the flow to supersonic as well as hypersonic speeds to seven different output Mach numbers. The interest was turned towards the variation of the minimum length of the divergent section in terms of the outlet Mach number. The authors [12] concluded that the length of the divergent section increases with the exit cross section Mach number and that the variation in length was not linear.

Plug and dual-bell nozzles actually considered by space industries and agencies as possible engine candidates for future supersonic rockets and space launchers thus calling for much study inherent to the improvement of their performances and reliability [13]. In a dual bell nozzle, two shortened bell-shaped configurations nozzles are joined together at an inflection point rendering it simple to design. The MoC is used to draw the base contour simulated as a 2nd-order

polynomial which was later truncated, while the profile of the second curve is calculated to give a constant wall pressure [14]. A similar investigation was carried out in terms of design of both bells of a dual bell nozzle using the MoC [15] and comparisons of the results were performed to experimental studies performed at the French 'Office National des Etudes et Recherches Aérospatiales-ONERA'.

The present investigation involves the development of a three-step procedure that enables the design of efficient TIC supersonic nozzles. It has been applied to the design of an IC then a TIC contour whose developed profiles along with their performance parameters have been computed and compared to results of similar studies.

2. MoC Design and simulation

An isentropic, 2-D, steady and irrotational flow may be expressed by the gas dynamic equation and the irrotationality condition represented by Equations (1) and (2) respectively.

$$\left(u^2-a^2\right)\frac{\partial u}{\partial x}+\left(v^2-a^2\right)\frac{\partial v}{\partial x}+2uv\frac{\partial u}{\partial y}-a^2\frac{v}{y}=0 \tag{1}$$

$$\frac{\partial u}{\partial y}-\frac{\partial v}{\partial y}=0 \tag{2}$$

Where (u) and (v) represent the axial and radial components of the velocity whereas (x) and (y) the axial and radial coordinate directions. The speed of sound is noted (a) whereas (δ) represents the kronecker symbol that allows the description of both a planar flow (δ=0) and an axisymmetric flow (δ=1).

The aforementioned partial differential equations are remodeled through the application of the MoC, given the appropriate boundary conditions, into ordinary differential equations known as the characteristic (Equation 3) and compatibility (Equation 4) relationships that are accessible to a numerical step-by step procedure that carries out computations along the Mach lines [17].

$$\lambda_{\pm}=\left.\frac{dy}{dx}\right|_{\pm}=tg\left(\theta\pm\alpha\right) \tag{3}$$

$$\left(u^2-a^2\right)du_{\pm}+\left[-\left(u^2-a^2\right)\lambda_{\pm}+2uv\right]dv_{\pm}-\left(\delta\frac{a^2v}{y}\right)dx_{\pm}=0 \tag{4}$$

Equation (3) represents the right-hand and left-hand characteristics defined by the subscripts (+) and (-). The slopes of the right- and left-hand characteristics are illustrated by (λ_+) and (λ_-) expressed in terms of the flow and Mach angles (θ) and (α) respectively. Integrated within a home-developed programme, the MoC was applied for the design of the supersonic nozzle that meets the required geometrical and thermodynamic specifications displayed in Table 1.

Table 1

Thermodynamic and geometrical inputs

Thermodynamic data	Geometrical data
P_a=1.013 (bars)	y_t=0.01 (m)
$P_t = 30$ (bars) T_t= 330 (K)	R_{tu}=0.03 (m) R_{td}=0.03 (m)
R_G=280 (J/kg.K)	θ_A=15 (°)
γ=1.4	θ_E=0 (°)
	X_E=0.109 (m)

2. 1. Supersonic Ideal Contour (IC) nozzle

The nozzle considered is represented by an ideal profile where the throat is constituted of an upstream and downstream arcs of circles of different radii of curvature (*Rtu* and *Rtd* respectively). The downstream circular arc is tangentially attached to a contour simulated by a 2nd-order quadratic polynomial wall at the attachment point noted "A" in Figure.1.

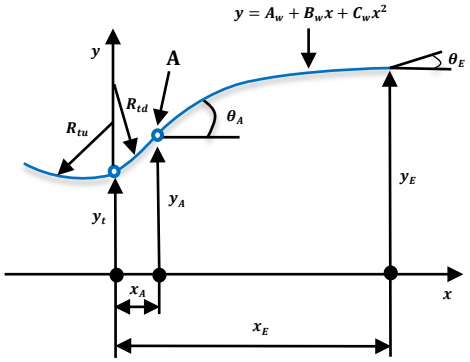

Fig. 1. Bell nozzle configuration

The boundary conditions set at the exit position (*E*) and obtained at the attachment point (*A*) enable the calculation of the three 2nd-order polynomial constants (A_w, B_w and C_w). The initiation of the supersonic computations necessitates the specification of the thermodynamic and geometrical data as shown in Table 1 [17].

The application of the numerical procedure of the characteristics generated the profile parameters represented by the nozzle radius at the exit, the coordinates of the attachment point and the coefficients describing the 2nd-degree polynomial wall are displayed in Fig. 2. These results are compared to those produced by a similar study performed at the 'Institut de l'Aéronautique et des Etudes Spatiales' of Blida-1 university [18]. The results of the comparisons are shown in Table 2.

Table 2

Profile comparison - Ideal nozzle.

Profile parameters	[17]	[18]
x_A (m)	0.007760	0.007764
y_A (m)	0.011020	0.011022
A_W	0.00886	0.00885
B_W	0.28843	0.29115
C_W	-1.31895	-1.51646
y_e (m)	0.02463	0.022919

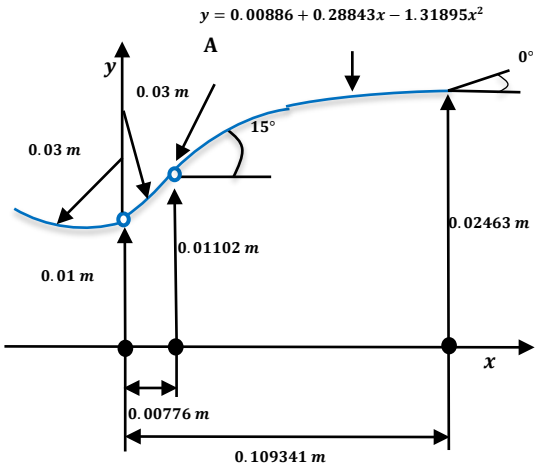

Fig. 2. Profile results for the Bell nozzle configuration

The obtained profiles are represented in Fig.3. Table 2 and Fig.2 show the similarity between the two contours particularly before the attachment point i.e. at the beginning of the expansion until approximately halfway of the divergent (at around x=0.05m) where they slightly diverge. This is mainly due to the difference in the results obtained in terms of the coefficients of the 2nd-degree polynomial describing the diverging section.

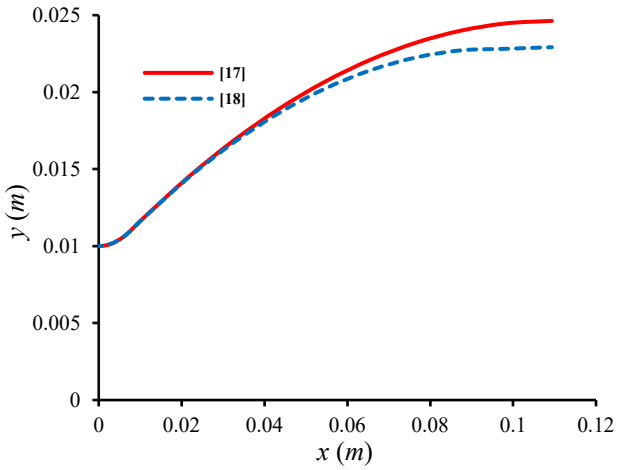

Fig. 3. IC Profiles-Divergent section

2. 2. Supersonic Truncated Ideal Contour (TIC)

A truncation is almost necessary to reduce an ideal nozzle weight without losing too much performance mainly in terms of thrust. A truncation at the desired cross-section would certainly lead to a loss due to exit flow divergence and hence exit velocity in the axial direction. However, and fortunately, this would be compensated by the weight gained. A 20% truncation has been reported as the best compromise between thrust loss and weight gain [18]. Performed on the IC nozzle and keeping the same geometrical and thermodynamic data, the length will decrease and the exit angle increase as is shown in Fig.4. Table 3 compares these paramers inherent to IC and TIC configurations.

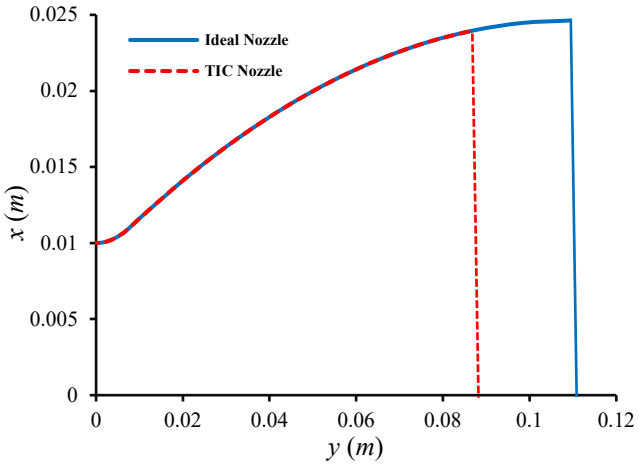

Fig. 4. IC Profiles -Divergent section. IC and TIC profiles

Table 3

Profile comparison - Ideal nozzle

Profile parameters	x_E (m)	θ_E (°)	y_E (m)
IC	0.109341	0	0.02463
TIC	0.08747	3.3	0.02400

2. 3. Convergent design approach

The profile of the complete nozzle was generated. The converging section, whose role is to make the flow achieve a Mach number of unity at the throat to be ble to start a supersonic expansion within the diverging section. The convergent was produced by applying the Rao approach [19]. It is linked to the upstream arc-of-circle of radius (R_{tu}). Being a result of numerous experimental investigations, the Rao's approach allows the design of the converging profile on the basis of the throat radius successfully.

$$\begin{cases} x = 1,5\ y_{col}\ \cos(\theta) \\ y = 1,5\ y_{col}\ \sin(\theta) + 2,5\ y_{col} \end{cases} \quad (5)$$

With: $-130° \leq \theta \leq -90°$

The calculations carried out by the authors led to the design of the convergent profile (Table 4) that will be linked to the diverging section thus constituting the entire converging-diverging nozzle. Fig. 8 illustrates the convergent profile section.

Table 4

Profile of the converging section

θ(°)	x (m)	y (m)
-90	0.	0.01
-95	-0.0013073361	0.0100570795
-100	-0.0026047227	0.0102278837
-105	-0.0038822857	0.0105111126
-110	-0.0051303021	0.0109046107
-115	-0.0063392739	0.0114053832
-120	-0.0075	0.0120096189
-125	-0.0086036465	0.0127127193
-130	-0.0096418141	0.0135093334

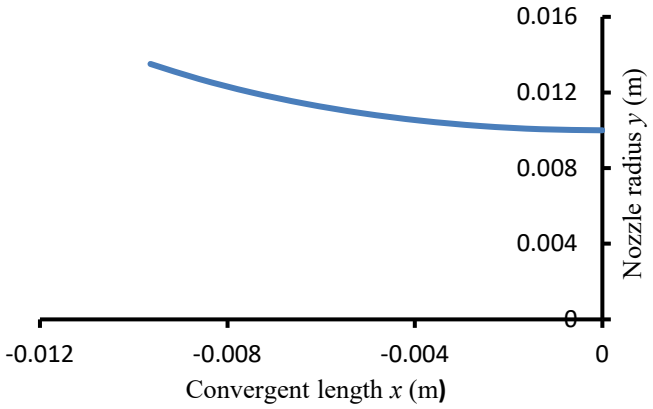

Fig. 5. Profile-Convergent section

2. 4. CFD approach

A CFD solver based on the finite volume method was applied for the simulation of the compressible flow field within the entire ideal contour nozzle. The computations were carried out on the Ansys-Fluent platform until a solution is reached within the optimal design conditions.

The computational domain is meshed using a regular and a structured grid of quadrilateral elements. It comprises 12,500 elements including 250 in the axial direction (x) and 50 along the radial direction (y). A more finely resolved mesh was employed in the vicinity of the throat where property gradients are expected to be higher as well as along the solid wall where the viscosity effects are prominent (Fig.6).

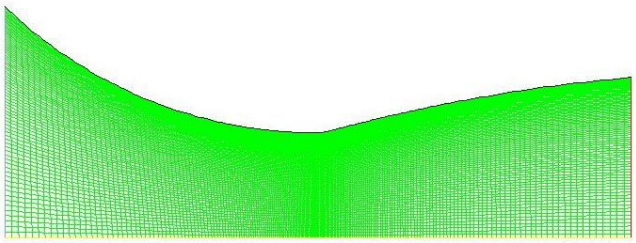

Fig. 6**.** Grid topology of the TIC nozzle

The governing equations include the physical laws pertaining to conservation of mass, momentum, and energy. The (k-ω) model was selected as the turbulent model. Table 5 summarizes the computational parameters applied in the simulation that led to obtaining the results shown in the tables and figures below.

Table 5

Simulation criteria

Features applieed	
Solver	Density based
Property	Ideal gas
Viscosity model	*k-ω*
Operational pressure	0
Inlet boundary conditions	30.10^5 Pa / 330 K
Outlet boundary conditions	$1.013.10^5$ Pa
Residuals	10^{-6}

3. Results and discussions

3. 1. Ideal Contour nozzle

The performances inherent to the IC nozzle configuration have been calculated and compared to those available in the literature [18]. The results are shown in Table 6, and are found close to within 6% in terms of the thrust coefficient that represents the efficiency of the expansion within the divergent section. The results obtained demonstrate the robustness of the configuration designed along with its ability to expand the gases efficiently.

Table 6

IC nozzle performance comparison

Performance parameters	[17]	[18]	Error (%)
T (N)	1513.01	1433.39	5.5
$\dot{m}$ (kg/s)	2.013	2.139	6.2
C_T (-)	1.61	1.52	5.9
M_e (-)	3.24	3.37	4.0
I_S (-)	71.267	68.32	4.3.

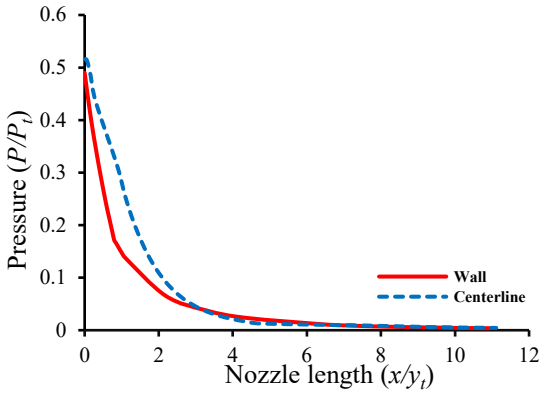

Fig. 7. Pressure distribution-IC nozzle

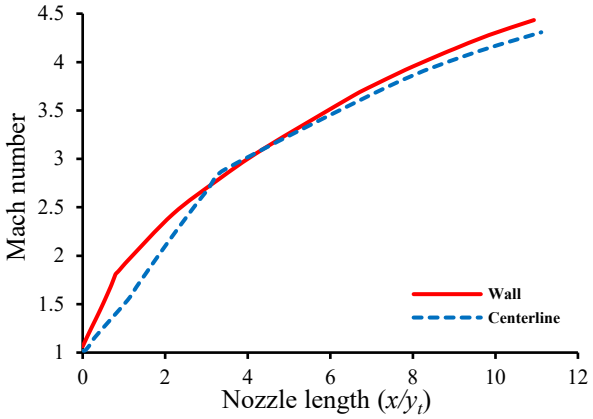

Fig. 8. Mach distribution-IC nozzle

Fig. 7 and Fig.8 show the evolutions of the static pressures and Mach along both the centerline and the wall. The sharp expansion, and therefore the severe decrease in terms of the pressure with the corresponding increase in Mach, may be noticed immediately downstream of the throat. These are the direct results of the high angle at the attachment point (A). The expansion becomes steadier afterwards as the profile is straightened up and the flow directed towards the axis of symmetry. This action tends to enhance the thrust in the axial direction.

3. 2 .Truncated Ideal Contour nozzle

The nozzle having been truncated, the transonic and supersonic flow-fields within the throat and divergent sections are re-calculated. The results obtained by applying the MoC are represented in terms of static pressure along the centerline and wall, and are shown in Fig.9.

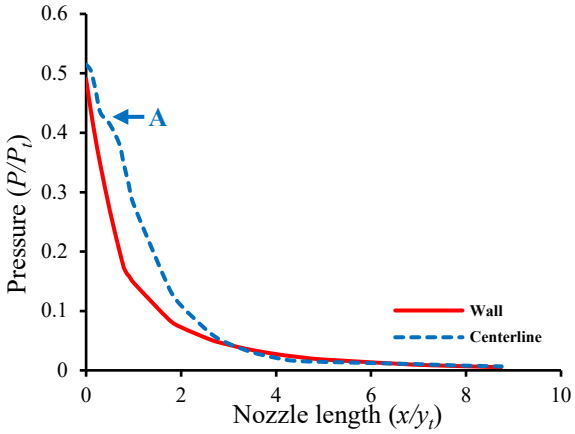

Fig. 9. Pressure distribution-TIC nozzle

A sharp expansion is noticed to take place immediately downstream of the throat before straightening up afterwards and heading towards the centerline optimizing the thrust in this direction. The expansion along the centerline shows a point of discontinuity noted 'A' in Fig.9. It represents the transition of the expansion process from the arc-of-circle located downstream of the throat to the polynomial wall profile. It displays the real character of the expansion in view of the fact that the MoC (as its name indicates) initiates its computations along the characteristics represented by the Mach lines in the particular case of the supersonic flow under consideration. This point of discontinuity does not appear on the curve representing the expansion along the wall because at this point, the Mach lines are either confounded or merged.

Furthermore, a comparison is undertaken between the IC and TIC profiles designed. They are displayed in Table 7 and show the similarities of the two configurations in terms of performance.

Table 7

IC-TIC nozzles comparison

Performance parameters	IC nozzle [17]	TIC nozzle
T (N)	1513.01	1333.2
$\dot{m}$ (kg/s)	2.013	2.0135
C_T (-)	1.61	1.41
I_S (-)	71.267	62.44

To visualize the flow field within the nozzle, a CFD simulation was carried out. Both the static pressure and Mach number have been computed and the results in terms of contours are presented in Fig.9 and Fig.10 respectively. The pressure (Fig. 10) is seen to be decreasing in a uniform way from its initial value of 30 bars at the convergent entry to an average of 0.5 bar at the exit. A significant decrease therefore representing a strong pressure gradient is observed immediately after the throat (represented in green in Fig. 10). It stabilizes further downstream with the flow direction tending to resume in the axial direction due to the decrease in the angle of divergence. It discharges almost axially i.e. in a direction parallel to the centerline thus resulting in maximum thrust in the axial direction.

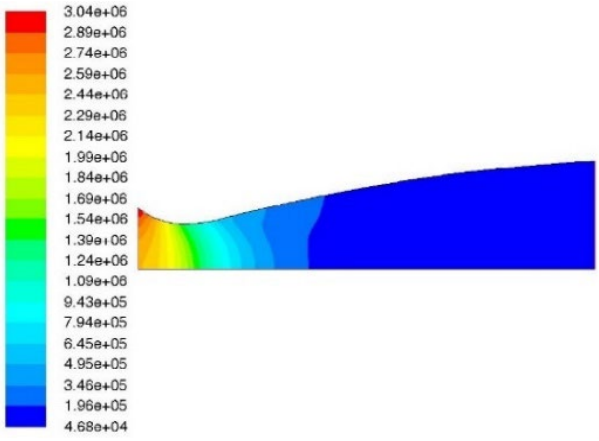

Fig 10**.** Pressure contour-TIC nozzle

Fig. 11 illustrates the Mach number contours along the diverse cross-sections of the truncated profile. An increase in Mach can be observed from the start of the converging section then through the throat where it reaches unity to be able to initiate a supersonic expansion within the divergent. The magnitude of the Mach number starts with M=0.08 at the entry to the convergent from the combustion chamber to achieve a value of M=3.3 at the exit cross-section.

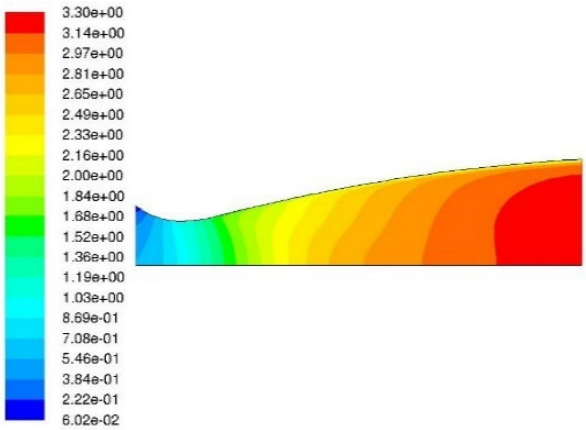

Fig. 11. Mach contour-TIC nozzle

The pressure distributions along the centerline and wall of the TIC configuration are displayed in Fig. 12. As a consequence of the viscosity effects that are predominant near the nozzle walls, The initial pressure at the wall is found to be lower than that at the centerline. It decreases sharply afterwards because of the abrupt expansion due to the large divergence attachment angle. Along the centerline, the flow is found to expand more uniformly.

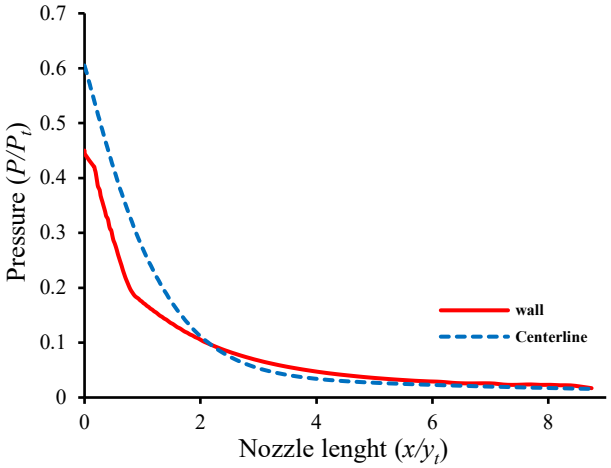

Fig. 12. Pressure distribution FVM-TIC nozzle

Figs 13 and 14 compare the results obtained through the application of the MoC and FVM approaches. A good agreement is achieved in terms of the pressure distribution along both the centerline (Fig. 13) and the wall (Fig. 14). A difference in terms of the initial pressure pertaining to the MoC and FVM results may be observed. It is essentially due to the fact that the MoC starts the computations downstream of the throat as it can only handle supersonic flows while the FVM approach computations have been applied along the entire nozzle i.e. the convergent, the throat and the divergent.

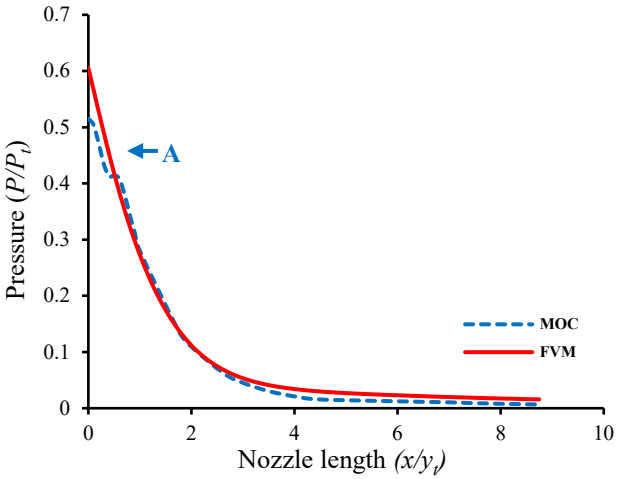

Fig. 13. Pressure distribution along the centerline-TIC nozzle

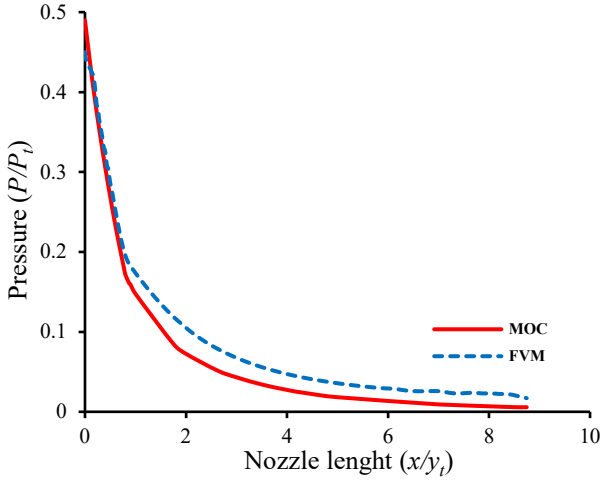

Fig. 14. Pressure distribution along the wall -TIC nozzle

As shown in Fig. 9 and explained afterwards, a point of discontinuity appears in the pressure distribution curve pertaining to the expansion along the centerline determined through the application of the MoC. It is also noted 'A' in Fig. 13 and displays the true character of the expansion computed along the Mach lines. It does not appear on the results of the Finite Volume Method procedure because they are smoothed out as a consequence of the interpolations performed during the computations carried out by the FVM method.

6. Conclusions

The design of a de-Laval contoured single-bell ideal contour (IC) nozzle has beeen carried out along with its truncation at a cross-section to achieve a Truncated Ideal Contour (TIC) profile have been performed. The truncation was implemented at 20% of the total length as it is reported to be the best compromise between thrust loss and weight gain. The simulations of the flow-field within the supersonic section of both configurations have been carried out using the MoC while the TIC nozzle flow-field was furthermore investigated through a CFD simulation. The performance parameters of the IC configuration have been compared to those obtained on both a similar application and to its TIC counterpart. The results achieved and comparisons performed lead to the following conclusions:

1. In the case of the IC configuration, the two profiles demonstrated a similar profile immediately downstream of the throat to approximately halfway through i.e. at approximatively $x \approx 0.05$m where they slightly diverge. This similarity immediately downstream of the throat is mainly due to the fact that the expansion within these sections is mainly governed by the circular-arc throat contour (R_{td})

while further downstream, the control is performed by the 2nd-order quadratic polynomial wall. Therefore, the slight discrepancy in the profile is in fact the result of the difference in terms of the polynomial constants A_w, B_w, and C_w describing the diverging section.

2. In terms of he computed performances, the IC nozzle delivered a thrust coefficient and a specific impulse close to that of the compared configuration. Agreement was obtained within 5.9% and 4.3% respectively.
3. The static pressure distribution representation along the wall and the centerline show a sharp expansion taking place immediately downstream of the throat i.e. right after the throat section and before the attachment point where the diverging angle is at its maximum. It tends to stabilize downstream to almost merge under the effect of the 2nd-order quadratic polynomial wall that reaches an angle of θ_E=0° at the exit cross-section. In terms of Mach, a similar increase takes place immediately after the throat and continues to reach a maximum value of M = 4.3 at the exit.
4. The TIC configuration was obtained through the truncation of its IC counterpart. MoC and Rao methods were applied to derive the divergent and convergent sections respectively.The Rao convergent profile was linked to the circular arc contour upstream of the throat. A 12,500-elements mesh was produced with refinements in the throat region and along the solid wall. The contours of both the static pressure and Mach were generated. They show the flow expanding smoothly without shock waves. A fairly large decrease in pressure accompanied by a corresponding increase in Mach are shown to take part immediately downstream of the throat tending to stabilize downstream with the decrease in the divergence angle.
5. In terms of pressure profiles generated by the two approaches, the results were found to be very close. The expansion along the centerline inherent to the MoC shows a point of discontinuity representing the transition from the throat downstream arc-of-circle to the polynomial profile showing the real nature of the expansion as the computations are carried out along the Mach lines. This discrepancy does not appear on the expansion curve of the wall as, at this point, the Mach lines are merged.

Acknowledgement

The present research has been undertaken at the 8 May 1945 university, Guelma-Algeria under the PRFU research project A11N01UN240120210001. The authors wish to acknowledge the contribution of the General Directorate of Scientific Research and Technological Development (DGRSDT) for their help and support.

REFERENCES

[1]. *J.D. Anderson*, "Modern compressible flow with historical perspective", McGraw-Hill Higher Education, New York, 2003, 3rd Edition.

[2]. *G.P. Sutton, and O. Biblarz*, "Rocket propulsion elements", Wiley India Pvt. Ltd., 2013, 7th Edition.

[3]. *S. Khare, and UK Saha*, "Rocket nozzles: 75 years of research and development", Sådhanå, 46:76, 2021, doi.org/10.1007/s12046-021-01584-6

[4]. *A. Bani*, "Design and analysis of an axisymmetric aerospike supersonic micro-nozzle for a refrigerant-based cold-gas propulsion system for small satellites", M.S. thesis, Missouri Univ. of Sc. And Tech-MUST, 2016.

[5]. *A. Haddad*, "Aérodynamique interne des prises d'air et tuyères supersoniques", cours, Institut d'Aéronautique et Etudes Spatiales, univ. Blida-1, 2000.

[6]. *E.C. Guentert, and H.E. Neumann*, "Design of Axisymmetric Exhaust Nozzles By Method of Characteristics Incorporating A Variable Isentropic Exponent", 1959, NASA Technical Report R-331959.

[7]. *M.J. Zukrow, and J.D. Hoffman*, 'Gas Dynamics', John Wiley & Sons, New York, 1976, **Vol. I-II**.

[8]. *A. Kumar, and S.G. Ogalapur*, "Design of Minimum length nozzle by Method of Characteristics", 2020, Int. J. of Sc. Engg and Technology, 8:6.

[9]. *M. Murnaghan*, "Study of minimum length, supersonic nozzle design using the Method of Characteristics", 2019, Master's Degree in Space and Aeronautical Engineering dissertation, Universitat Polit`ecnica de Catalunya, Spain.

[10]. *B.D. Baloni, S.P. Kumar, and S.A. Channiwala*, "Computational Analysis of Bell Nozzles", 2017, Proc. of the 4th Int. Conf. of Fluid Flow, Heat and Mass Transfer (FFHMT'17), Toronto, Canada Paper No. 110, doi.org/10.11159/ffhmt17.110.

[11]. *L. Silwal, S. Sharma, N. Acharya, and S. Bhattrai*, "Design and numerical analysis of asymmetric nozzle of shcramjet engine", Int. J. of Aerospace and Mechanical Engg, vol. 3, n°6, 2016.

[12]. *V. Ramji, R. Mukesh, and I. Ha*san, "Design and numerical simulation of convergent divergent nozzle", Applied Mechanics and Materials, vol. 852 (2016) 617-624, doi:10.4028/www.scientific.net/AMM.852.617.

[13]. *G. Hagemann, H. Immich, T.V. Nguyen and G.E. Dumnov*, Advanced rocket nozzles, Journal of Propulsion and Power, 14(5) (1998) 620-634.

[14]. *H. Kbab, M. Sellam, T. Hamitouche, S. Bergheul and L. Lagab, L*. Design and performance evaluation of a dual bell nozzle, Acta Astronautica, 130 (2017) 52-59.

[15]. *T. Hamitouche, M. Sellam, H. Kbab and S. Bergheul*, Design and wall Fluid parameters evaluation of the dual-bell Nozzle, Int. J. Eng. Research Technology, 12:7 (2019) 1064-1074.

[16]. *N. Boughazi and A. Haddad*, "A Simple Method for the Design of Supersonic Nozzles of Arbitrary Cross Section Shape", ASME Fluids Engineering Division Summer Meeting, 2020, https://doi.org/10.1115/FEDSM2020-20197

[17]. *M. Laib*, Approches par caractéristiques et volumes finis de l'écoulement au sein de tuyères de Laval-Application à une tuyère cloche à simple galbe, Master thesis, Guelma Univ. (2020).

[18]. *T. Hamitouche and O. Djebbar*. Développement d'une méthode de conception de profil de tuyère double galbe (dual-bell nozzles), Master thesis, IAES, Blida-1 Univ. (2014).
[19]. *UYEKI, Devyn Yoshio Kapukawai*. A Design Method for a Supersonic Axisymmetric Nozzle for Use in Wind Tunnel Facilities. MSc in Aerospace Engg, Dept of Aerospace Engg, Dan José University, 201